

# EFFECT OF THE TOOL GEOMETRY AND WELDING PARAMETERS ON THE MACROSTRUCTURE, FRACTURE MODE AND WELD STRENGTH OF FRICTION-STIR SPOT-WELDED POLYPROPYLENE SHEETS

## VPLIV GEOMETRIJE ORODJA IN PARAMETROV VARJENJA NA MAKROSTRUKTURO, VRSTO PRELOMA IN TRDNOST ZVARA PRI TORNO-VRTILNEM TOČKASTEM VARJENJU POLIPROPILENSKIH PLOŠČ

**Mustafa Kemal Bilici<sup>1</sup>, Ahmet İrfan Yüklér<sup>1</sup>, Alim Kastan<sup>2</sup>**

<sup>1</sup>Department of Materials Technology, Marmara University, 34722 Istanbul, Turkey

<sup>2</sup>Department of Materials Technology, Afyon Kocatepe University, 03200 Afyon, Turkey  
mkbilici@marmara.edu.tr

*Prejem rokopisa – received: 2013-10-05; sprejem za objavo – accepted for publication: 2013-11-19*

The effect of the tool geometry and welding parameters on the macrostructure, fracture mode and weld strength of the friction-stir spot welds of polypropylene sheets was studied. Three fracture modes were observed: the nugget pull-out failure, the cross-nugget failure and the mixed nugget failure under a lap-shear tensile test and nugget debonding and a pull out under a cross-tension loading, while the lap-shear tensile load was not affected significantly by the delay time. The lap-shear tensile load and the nugget thickness increased with the increasing tool rotation speed and dwell time. The macrostructure shows that the welding parameters have a determinant effect on the weld strength ( $x$ : the nugget thickness,  $y$ : the thickness of the upper sheet). Finally, when different welding parameters were used, different fracture modes of the joints were obtained in the friction-stir spot welding of polypropylene sheets. Based on the experimental observation of the macrostructures, the effect of the welding parameters and tool geometry on the lap-shear tensile load and the fracture mode were discussed.

**Keywords:** polymers (thermoplastics), polypropylene, friction-stir spot welding, polymer welding, welding parameters

Preučevan je bil vpliv geometrije orodja in parametrov varjenja na makrostrukturo, vrsto preloma in trdnost zvara pri tornu-vrtilnem točkastem zvaru polipropilenskih plošč. Opaženi so trije načini preloma: porušitev z izpuljenjem jedra, porušitev s pretgom jedra in mešan prelom jedra pri prekrivnem strižnem preizkusu ter prekinitve v jedru in izpuljenje jedra pri prečni natezni obremenitvi, medtem ko na prekrivno natezno obremenitev ni bilo velikega vpliva. Prekrivna strižna napetost in debelina jedra sta naraščali z naraščanjem rotacijske hitrosti orodja in časa zadržanja. Makrostruktura kaže, da parametri varjenja igrajo pomembno vlogo pri trdnosti zvara ( $x$ : debelina jedra,  $y$ : debelina zgornje plošče). Končno, če so bili uporabljeni različni parametri varjenja, so bili različni tudi načini porušitve pri tornu-vrtilnem točkastem varjenju polipropilenskih plošč. Na osnovi eksperimentalnih opažanj makrostrukture je prikazan vpliv parametrov varjenja in geometrije orodja na prekrivno strižno natezno obremenitev in vrsto preloma.

**Ključne besede:** polimeri (termoplasti), polipropilen, tornu-vrtilno točkasto varjenje, varjenje polimera, parametri varjenja

## 1 INTRODUCTION

Recently, a new joining technique called friction-stir spot welding (FSSW) or friction spot joining (FSJ) has been developed<sup>1</sup>. This technique has the same advantages as friction-stir welding (FSW) such as the solid-state process, ease of handling, joining of dissimilar materials and the materials that are difficult to fusion weld, a low distortion, excellent mechanical properties and little waste or pollution. Hence, it is expected to be used for joining lightweight materials in order to achieve a high performance and save the energy and costs of the machines.

The FSSW process consists of three phases: plunging, stirring and retracting<sup>2</sup>. The process starts with the spinning of a tool at a high rotation speed. Then the tool is forced into the workpiece until the shoulder of the tool plunges into the upper workpiece. The plunge movement of the tool causes the material to be expelled. When the

tool reaches the predetermined depth, the plunge motion ends and the stirring phase starts. In this phase, the tool rotates in the workpieces without plunging. Frictional heat is generated in the plunging and stirring phases and, thus, the material adjacent to the tool is heated and softened. The softened upper and lower workpiece materials mix together in the stirring phase. The shoulder of the tool creates a compressional stress on the softened material. A solid-state joint is formed in the stirring phase. When a predetermined bonding is obtained, the process stops and the tool is retracted from the workpieces. The resulting weld has a characteristic keyhole in the middle of the joint created during the friction-stir spot welding. Different welding-parameter configurations and their consequences on the weld strength and fracture mode can be identified. FSSW has been successfully applied to aluminium<sup>3</sup>, magnesium<sup>4</sup> and steel sheets<sup>5</sup>, but there are very few publications on its applications to polymer<sup>6-9</sup>.

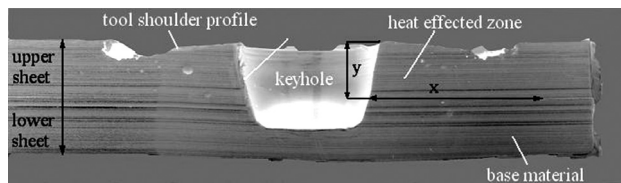


**Figure 1:** Schematic illustration of the cross-section of a friction-stir spot weld ( $x$ : nugget thickness,  $y$ : the thickness of the upper sheet and  $t$ : the total material thickness)

**Slika 1:** Shematski prikaz prereza tornjo-vrtilnega točkastega zvara ( $x$ : debelina jedra,  $y$ : debelina vrhnje plošče in  $t$ : skupna debelina materiala)

Based on the observations of the FSSW macrostructures, the weld zone of a FSSW joint is schematically illustrated in **Figure 1**. From the appearance of the weld cross-section, two particular points can be identified<sup>10</sup>. The first point is the thickness of the weld nugget ( $x$ ) which is an indicator of the weld-bond area (**Figure 1**). The weld-bond area increases with the nugget thickness. The second point is the thickness of the upper sheet under the shoulder indentation ( $y$ ). The sizes of these points determine the strength of a FSSW joint.

In this study, FSSW was performed to join PP sheets in order to understand the influence of the welding parameters and tool geometry on welds. The modifications of the macrostructural features (the fracture mode, the nugget thickness and the thickness of the upper sheet) induced by these different processing configurations are identified and their consequences on the weld strength and fracture mode during the lap-shear tensile tests are discussed. The purpose of this investigation was to improve the strength of the spot welds. Both the nugget thickness and the upper-sheet thickness have significant effects on the fracture modes under tensile loading.

## 2 EXPERIMENTS

In this investigation 4-mm-thick polypropylene sheets were used. The polypropylene sheets were purchased from SIMONA AG, Germany (the tensile yield stress of 34 MPa or lap-shear fracture load of 4500 N). Specimens were made by using 60 mm by 150 mm sheets with a 60 mm by 60 mm overlap area. In order to carry out the FSSW tests, a properly designed clamping feature was utilized to fix the specimens to be welded on an NC milling machine. The tool was made of the SAE 1040

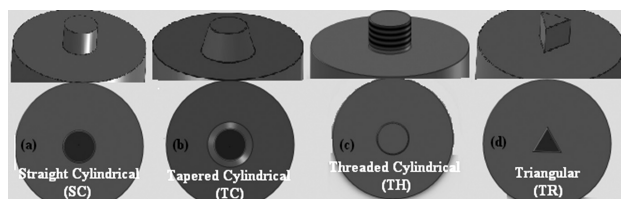


**Figure 2:** FSSW tool profiles: a) straight cylindrical, b) tapered cylindrical, c) threaded cylindrical, d) triangular

**Slika 2:** Profil FSSW-orođja: a) raven valjast, b) stožčast valjast, c) valjast z navojem, d) trikoten

steel and heat-treated to a hardness of 35 HRC. Four different tool-pin profiles (straight cylindrical, tapered cylindrical, threaded cylindrical and triangular) were used to fabricate the joints (**Figure 2**).

Each tool had a pin length 5.5 mm and pin size 7.5 mm. The tapered pin had a 15° pin angle. For the straight cylindrical, tapered cylindrical and threaded cylindrical pins, the pin size was determined by measuring the bottom diameter of the pin. For the triangular pins, the pin size was determined by calculating the diameter of the cross-section area formed by the turning pin.

In all the cases, the constant tool-plunge rate of 0.26 mm/s and the shoulder-plunge depth of 0.2 mm below the upper-plate surface were applied. The tool rotation speeds and the tool dwell times also varied, being between 560 r/min and 1400 r/min, and between 20 s and 200 s, respectively.

The welded lap-shear specimens were tested on a ZWICK machine at the constant cross-head speed of 5 mm/s. The load and displacement were simultaneously recorded during the test. The fracture mode of each specimen was then determined. The fracture-mode-appearance observations of the joints were done with a camera. For the weld-macrostructure studies, thin slices (of 20  $\mu\text{m}$ ) were cut from the welded specimens using a Leica R 6125 rotary microtome. These thin slices were investigated using a video spectral comparator. The photographs of the cross-sections were obtained.

## 3 EXPERIMENTAL RESULTS

During the FSSW of polypropylene, three types of fracture mode were observed as shown in **Figure 3**: (a) the nugget pull-out failure,  $P$ ; (b) the cross-nugget failure,  $C$ ; and (c) the mixed nugget failure,  $M$ . By changing the welding parameters, these three types of fracture mode were changed. These three types of fracture mode are affected by the heat amount: insufficient heat, ideal heat and excessive heat. Consequently, the orientation of the fracture mode changes the weld strength. While the highest lap-shear fracture load causes a nugget pull-out

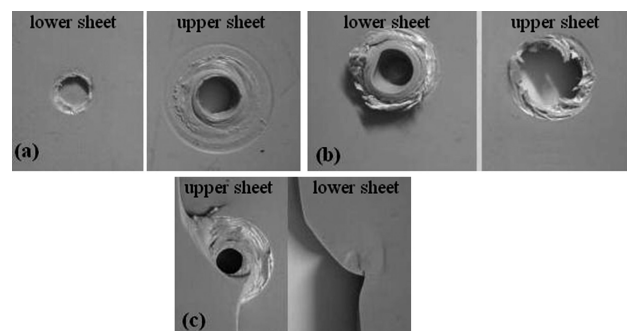


**Figure 3:** Three types of fracture mode: a) nugget pull-out failure, b) cross-nugget failure and c) mixed nugget failure

**Slika 3:** Tri vrste preloma: a) izvlečenje jedra, b) prečna porušitev jedra in c) mešana porušitev jedra

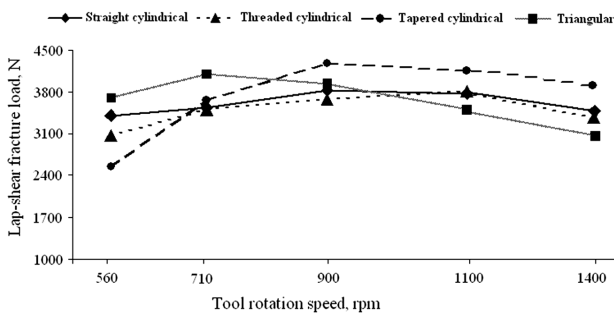


**Figure 4:** Effect of tool profile and tool rotation speed on weld strength

**Slika 4:** Vpliv profila orodja in hitrosti vrtenja orodja na trdnost zvara

failure, the lowest lap-shear load causes a cross-nugget failure.

The effect of the tool-pin geometry on the lap-shear fracture load is shown in **Figure 4**. In these tests the welding parameters were kept constant: the tool rotation speed ranged from 360 r/min to 1400 r/min, the tool-plunge rate was 0.26 mm/s, the dwell time was 120 s and the tool-plunge depth was 5.7 mm. The maximum fracture load (900 r/min) was obtained with the tapered cylindrical pin (4280 N) and the threaded cylindrical pin resulted in the lowest fracture load (3305 N). Due to the maximum fracture load obtained with the tapered cylindrical pin, all the experiments were made with the tapered cylindrical pin. The effect of the tool profile on the welding zone is shown in **Figure 5**. The three photographs illustrate that the size of the keyhole formed in the welding zone depend directly on the pin profile. The

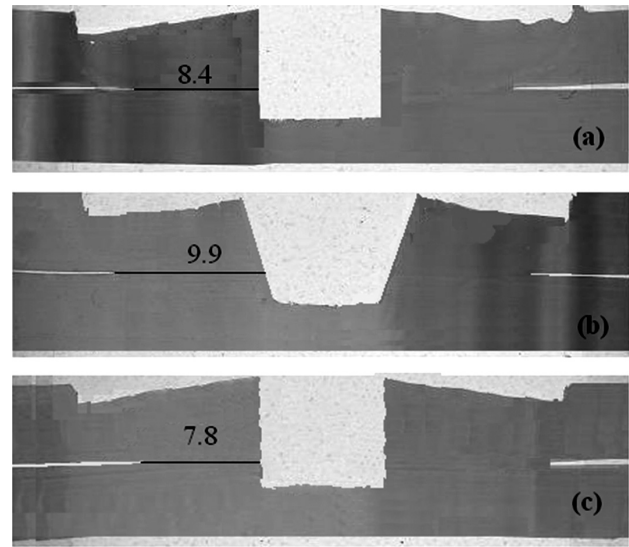


**Figure 5:** Effect of tool geometry on weld-nugget formation: a) straight cylindrical pin, b) 15° angled tapered cylindrical pin and c) threaded cylindrical pin

**Slika 5:** Vpliv geometrije orodja na nastanek jedra: a) cilindrična konica, b) stožčasta valjasta konica s kotom 15° in c) valjasta konica z navoji

wall slope of the keyhole changed with the pin-angle of the tool. The nugget thickness was 8.4 mm for the straight cylindrical pin, 9.9 mm for the 15° angled tapered pin and 7.8 mm for the threaded cylindrical pin. The tapered pin created a thicker nugget and a bigger weld-bond area than the straight cylindrical pin. The nugget thickness increased with the pin profile changes, as shown in **Figure 5**. Also, the nugget thickness exhi-

**Table 1:** Effect of tapered cylindrical pin on the fracture mode and nugget thickness

**Tabela 1:** Vpliv valjaste konice na način preloma in debelino jedra

Tool rotation speed (r/min)	Fracture mode	Macrostructure	Quality of weld-metal consolidation	Probable reason for the formation
360			very poor	Insufficient flow of the joining materials due to low heat
560			poor	Although there was insufficient heat, a weld was formed
710			better than in the previous case	Heat input is sufficient for a good-quality weld
900			very good	Heat input is sufficient for a good-quality weld
1120			good	Heat input is sufficient for a good-quality weld
1400			worse than in the previous case	Poor weld quality occurred due to excessive heat

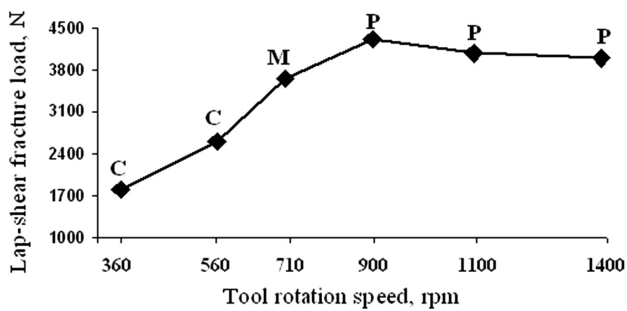


**Figure 6:** Effect of tapered cylindrical pin on lap-shear fracture load  
**Slika 6:** Vpliv stožčasto valjaste konice na prekrivno strižno obremenitev

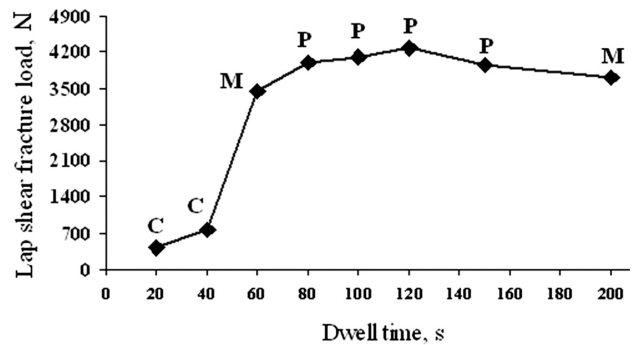


**Figure 7:** Effect of dwell time on lap-shear fracture load  
**Slika 7:** Vpliv časa zadržanja na prekrivno strižno obremenitev

bited a very large decrease with the threaded cylindrical pin, as shown in **Figure 5**.

The best results were obtained in the experiments involving the tapered cylindrical pin. For this reason, for the following experiments, investigating the effect of the welding parameters the tapered pin was used. In order to determine the effect of the tool rotation speed on the FSSW of polypropylene, seven different speeds were used. For all the welds, the plunge rate was 0.26 mm/s, the dwell time was 120 s and the tool-plunge depth was 5.7 mm. These three parameters were kept constant and only the dwell time was allowed to vary in the welding operations. Increasing the tool rotation speed from 360 r/min to 1400 r/min resulted in a linear progress in the strength of the welds. The effects of these speeds are shown in **Figure 6**. While the lap-shear fracture load dramatically increased up to the rotation speed of 900 r/min, it decreased after 900 r/min. The maximum fracture load obtained at 900 r/min was 4280 N. The fracture modes obtained were the cross-nugget failure at the speeds of 360 r/min and 560 r/min, the nugget pull-out failure at 710 r/min, and the mixed nugget failure at (900, 1120 and 1400) r/min. The fracture mode and the macrostructure are shown in **Table 1**.

The largest nugget thickness was 9.9 mm obtained at the tool rotation speed of 900 r/min. The lowest nugget thickness was 4.5 mm obtained at the tool rotation speed

of 360 r/min. This nugget thickness is very important for the lap-shear fracture load. At the tool rotation speed of 900 r/min, a thicker nugget and a larger weld-bond area than at the other tool rotation speeds were obtained. The nugget thickness and the fracture load increased with the tool rotation speed as shown in **Table 1** and **Figure 6**.

**Figure 7** shows the effect of the dwell time on the lap-shear tensile strength of FSSW joints. For all the welds, the plunge rate was 0.26 mm/s, the tool rotation speed was 900 r/min and the plunge depth was 5.7 mm. These three parameters were kept constant and only the dwell time was allowed to vary during the welding operations. The dwell-time experiments used the tapered pin. Increasing the dwell time from 20 s to 180 s resulted in a linear progress in the strength of the welds. The transition time for the failure modes of the PP sheets 4 mm under the above-mentioned welding parameters was found to be 45 s. In the period between the dwell times of 20 s and 120 s, there was a slight increase in the weld strength. For the dwell times of more than 120 s, the lap-shear fracture load showed a linear decrease after 120 s. A longer tool stirring time did not affect the weld strength. Only the fracture mode was changed during the lap-shear tests. The effect of the dwell time on the weld cross-sections is shown in **Table 2**. A thin nugget of the weld developed over the dwell time of 20 s (**Table 2**). The nugget thickness increased with the dwell time

**Table 2:** Influence of dwell time on the fracture mode and nugget thickness

**Tabela 2:** Vpliv časa zadržanja na vrsto preloma in debelino jedra

Dwell time (s)	Fracture mode	Macrostructure	Quality of weld-metal consolidation	Probable reason for the formation
20			very poor	Insufficient flow of the joining materials due to low heat
120			very good	Heat input is sufficient for a good-quality weld
200			worse than in the previous case	Poor weld quality due to excessive heat

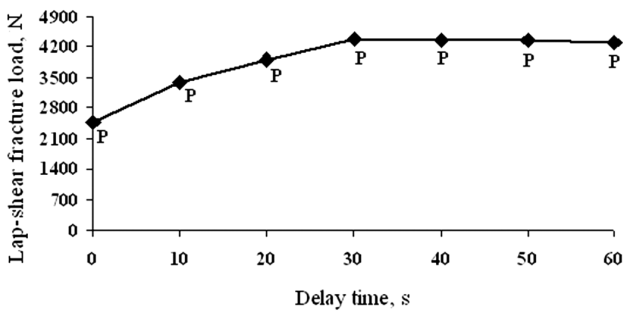


**Figure 8:** Effect of delay time on lap-shear fracture load  
**Slika 8:** Vpliv časa zakasnitve na prekrivno strižno obremenitev

(Table 2). The maximum fracture load was obtained at the dwell time of 120 s. Different fracture modes were obtained during the dwell-time tests: the cross-nugget failure at the dwell times of 20 s and 45 s; the pull-nugget failure at the dwell times of (80, 100, 120 and 150) s; and the mixed nugget failure at the dwell times of 60 s and 200 s. The fracture mode and the macrostructure are shown in Table 2. The largest nugget thickness was 9.9 mm obtained at the dwell time of 120 s. The smallest nugget thickness was 1.1 mm obtained at the dwell time of 20 s. The dwell time is very important for the nugget thickness. At the dwell time 120 s, a thicker nugget and a bigger weld-bond area were produced than at the dwell times 20 s and 200 s, as shown in Table 2.

In order to determine the effect of the delay time on the FSSW of polypropylene, seven different delay times were used. Figure 8 shows the effect of the delay time on the weld strength. In all the welds, the plunge rate was 0.26 mm/s, the dwell time was 120 s and the plunge depth was 5.7 mm. These three parameters were kept constant and only the dwell time was allowed to vary during the welding operations. The lap-shear fracture load was on an increase up to the dwell time of 30 s. After this dwell time, the lap-shear fracture load decreased very little. Although the delay time increased up to seven fold, the weld strength changed only within the experimental scatter limits (delay times of (0, 10, 20) s). The highest lap-shear fracture load was obtained after 30 s. For all the delay times the fracture mode was observed to be the nugget pull-out failure. The largest nugget thickness was 9.9 mm obtained with the delay time of 45 s. The delay time is very important for the

nugget thickness. The delay time 45 s led to a thicker nugget and a bigger weld-bond area than the delay times of 0 s to 30 s, as shown in Table 3.

#### 4 DISCUSSION

The importance of the tool pin profile is shown in Figure 4. The tapered cylindrical pin resulted in the biggest and the threaded cylindrical pin resulted in the lowest lap-shear fracture load. The reason for this difference can be easily explained with the weld-nugget thicknesses that are shown in Figure 5. The straight cylindrical pin and tapered cylindrical pin have the same pin size (7.5 mm), but the weld-nugget thicknesses obtained with these pins are different. The nugget thickness obtained with the straight cylindrical pin was 8.4 mm as shown in Figure 5a. The tapered cylindrical pin provided the weld-nugget thickness of 9.9 mm (Figure 5b). The threaded cylindrical pin provided the weld-nugget thickness of 7.8 mm (Figure 5c). The tapered pin created a thicker nugget and a bigger weld-bond area than the other tools. With the straight cylindrical pin a small amount of frictional heat was produced in the weld; therefore, a small weld-bond area and a very low strength were obtained. The stirring of the pin increased with the tool rotation speed<sup>11</sup>. The frictional heat also increased with the rotation speed. The maximum strength was obtained with the speed 900 r/min. The welding residual stresses of the upper sheet increased with the tool rotation speed<sup>12</sup>. When the rotation speed exceeded 900 r/min, the strength decreased because of the increased residual stresses. The lap-shear fracture load of a FSSW joint is directly proportional to the nugget thickness and the weld-bond area<sup>10</sup>. The tapered pin produced more frictional heat and a larger weld thickness, as shown in Figure 5. The heat produced in the weld area is directly proportional to the welding parameters and the tool geometry<sup>13</sup>. Suitable welding parameters produce more heat and a large weld area, causing a high weld strength<sup>14</sup>. Therefore, the tapered pin produces a higher lap-shear fracture load than the other pins. As seen in Figure 4, the strength varies significantly with the tool pin profile. Figure 5 shows that the maximum nugget thickness (9.9 mm) changes with the pin profile. In fact, a change in the pin profile results in a more extensive stirring and a higher heat input during the

**Table 3:** Influence of delay time on the fracture mode and nugget thickness  
**Tabela 3:** Vpliv časa zakasnitve na vrsto preloma in debelino jedra

Delay time (s)	Fracture mode	Macrostructure	Quality of weld-metal consolidation	Probable reason for the formation
0			very poor	Insufficient flow of the joining materials due to low heat
45			very good	Heat input is sufficient for a good-quality weld

FSSW, causing the nugget thickness to develop. The shear fracture of the nugget takes place easily when the nugget thickness is small, having a low tensile-shear strength. The results presented in **Figure 5** are in agreement with the work up to a certain tool profile (tapered pin). Different tool profiles resulted in three types of fracture in the FSSW of PP. These three types of fracture mode are affected by the heat amount: insufficient heat, ideal heat and excessive heat. Consequently, frictional heat occurred with different tool profiles. The fracture-mode changes associated with the nugget thickness and weld strength are shown in **Figure 5**. As a result, the reason for this strength difference is the chain scission<sup>15</sup>. The chain scission lowers the strength of a thermoplastic material<sup>16</sup>. If a molten thermoplastic material is heated to a high temperature and then a high pressure is applied to it, a decrease in the molecular weight of the material occurs<sup>15</sup>. The mechanical properties of thermoplastics decrease with lowering the molecular weight<sup>17</sup>. In FSSW the welding tool produces a compressive pressure in the weld zone<sup>18</sup>. In the FSSW of thermoplastics, the material in the weld area melts<sup>7</sup>.

**Figure 6** shows the effect of the tool rotation speed of the tapered pin on the weld strength. The lowest strength was obtained at the tool rotation speed of 360 r/min. In this weld, a small amount of frictional heat was produced; therefore, a small weld-bond area, a very low strength and the cross-nugget failure were obtained. The stirring of the pin increased with the tool rotation speed<sup>13</sup>. The frictional heat increased with the rotation speed. The maximum strength (4280 N) was obtained with the speed 900 r/min. The welding residual stresses of the upper sheet increased with the tool rotation speed<sup>12</sup>. When the rotation speed exceeded 900 r/min, the strength decreased because of the increased residual stresses. The fracture mode changed with the increasing tool rotation speed. The fracture mode changed due to the frictional heat. The lowest frictional heat led to the cross-nugget failure, while the excessive frictional heat led to the mixed nugget failure (**Table 1**). A high frictional heat causes a high material temperature in the welding zone<sup>7</sup> and a thicker nugget, as shown in **Table 1**. The fracture also occurs due to the high frictional heat in the welding zone. The tapered pin forms a thicker nugget and a bigger weld-bond area than the other pins. In the FSSW fracture experiments, the ideal fracture type is the nugget pull-out failure due to the high weld strength.

**Figure 7** shows the effect of the dwell time of the tapered pin on the weld strength. The effects of the dwell time on the weld strength and fracture mode are shown in **Table 2**. Short dwell times cause a thin nugget thickness and the cross-nugget failure, as shown in **Table 2**. The nugget thickness, bond area and fracture mode have a direct effect on the weld strength. Increasing the dwell time from 20 s to 40 s resulted in a linear progress in the strength of the welds. All these welds were fractured under small tensile loads because of the small weld-bond

areas. As the dwell time increased, the frictional heat increased as well. Larger weld nuggets were obtained with longer dwell times, increasing the joint strength (**Table 2**). An increase in the dwell time changed the fracture mode. The maximum weld strength was obtained with the nugget pull-out failure, as shown in **Figure 7** (dwell time 120 s). The shape of the weld-bond area in FSSW is found to be of high importance. The weld nugget represents the weld bond in FSSW. The cross-section area of a weld nugget determines the strength of a weld<sup>19</sup>. Very high temperatures were recorded in the FSW of plastics<sup>8,12</sup>. High melt temperatures and high welding forces cause chain scission in the welding zones of the plastics, decreasing the weld strength<sup>20</sup>. The physical properties of a polymer are strongly dependent on the size or length of the polymer chain. For example, if a chain length is increased, the melting and boiling temperatures increase quickly as well. The weld strength also tends to increase with the chain length, as does the viscosity, or the resistance to flow, of the polymer in its melt state. The FSSW process produces high temperature and pressure. But the excessive heat and pressure cause the chain structure to break. Most of the molten material is expelled, so a very small weld stir zone is formed, resulting in a very small fracture load. Thus, a reduction in the weld strength occurs. In friction-stir welding it is very important to check the excessive heat and pressure. Furthermore, the tool geometry is very important in the production of heat and pressure.

In this study each mechanical-test diagram shows an extremum. The lap-shear fracture load increases with the tool rotation speed (**Figure 6**), the dwell time (**Figure 7**) and the delay time (**Figure 8**). All these diagrams indicate that there is an optimum value for each welding parameter. When a variable value exceeds the critical value, the weld strength starts to decrease. The size of the weld increases continuously with the welding-parameter variables (**Figures 6, 7 and 8**). For example, the weld-nugget thickness increases with the tool rotation speed (**Figure 6**). The lap-shear fracture load reaches its highest value with the tapered pin (**Figure 6**). The reason for this strength difference is the mechanical scission<sup>15</sup>. Mechanical scission lowers the strength of a thermoplastic material<sup>16</sup>. If a liquid thermoplastic material is heated to a high temperature and then a high pressure is applied to it, a decrease in the molecular weight of the material occurs<sup>15</sup>. The mechanical properties of thermoplastics decrease with lowering the molecular weight<sup>17</sup>. In FSSW the welding tool produces a compressive pressure in the weld zone<sup>18</sup>. In the FSSW of thermoplastics, the material in the weld area melts<sup>21</sup>. High liquid temperatures and high welding forces cause mechanical scission in the welding zones of the plastics, which lowers the weld strength<sup>20</sup>.

The frictional heat produced in the vicinity of the tool increased with the dwell time<sup>11,22</sup>, so the temperature of

the material increased as well. The temperature of the material reached the melting temperature (131 °C) in the dwell time 45 s. The temperature rose up to 142 °C within the dwell time 50 s and it did not change with the extended dwell time. Similar temperatures were calculated for the friction-stir welding of PP sheets<sup>12,22</sup>. If the tool was retracted at the end of the predetermined dwell time, the liquid filled the space of the pin, as shown in **Table 3**. This weld does not have a characteristic keyhole in the nugget. If the pin was retracted with the delay time 45 s, the liquid in the vicinity of the pin cooled down and solidified. Such a weld has a keyhole as shown in **Table 3**. During all the experiments, the nugget pull-out failure occurred at the end of the delay time. Also, an increase in the delay time increases the weld strength. The dwell times from 30 s to 60 s resulted in a linear progress in the strength of the welds. All these welds were fractured with small tensile loads because of the small weld-bond areas. Larger weld nuggets were obtained with longer delay times, which increased the joint strength (**Figure 8**). The shape of a weld-bond area in FSSW is found to be of high importance. The cross-section area of a weld nugget determines the strength of a weld<sup>23</sup>. A weld with a small bond area fractures under a low tensile force in the zero delay time. In the FSSW of PP sheets 4 mm, the ideal delay time was found to be 45 s.

Fracture modes were changed in accordance with the welding parameters and tool geometry. This change in the welds causes the melting and boiling temperatures to increase quickly. For example, as a chain length is increased, the melting and boiling temperatures increase quickly. The weld strength also tends to increase with the chain length, as does the viscosity, or resistance to flow, of the polymer in its melt state. Due to these properties of polypropylene, the weld strength and fracture mode can be changed. Therefore, in the FSSW of polypropylene, both the fracture mode and the weld strength were very important.

## 5 CONCLUSIONS

The macrostructures, the weld strength and the fracture mode of friction-stir spot welds of polypropylene sheets were investigated.

- In the FSSW of polypropylene, three types fracture mode were observed: the nugget pull-out failure, the cross-nugget failure and the mixed nugget failure.
- The weld strength during FSSW was found to mainly depend on two macrostructural features: the weld-nugget thickness ( $X$ ) and the thickness of the upper sheet under the shoulder indentation ( $Y$ ).
- With the increasing rotation speed (up to 900 r/min), the lap-shear fracture load decreased because of the increased amount of the heat generated by the mechanical scission in the stir zone.
- The tool rotation speed and dwell time must be sufficient to allow a high weld strength and the appropriate fracture mode.
- During the FSSW of polypropylene, the pin geometry affects the nugget formation and lap-shear fracture load.
- The optimum tool for sheets 4 mm was found to be the tapered cylindrical pin.
- Mechanical scission can occur during the FSSW of polypropylene, if excessive frictional heating is created in the weld zone, so the optimum welding parameters should be chosen (the tool rotation speed of 900 r/min, the dwell time of 120 s and the delay time of 45 s).

## 6 REFERENCES

- <sup>1</sup> Y. Tozaki, Y. Uematsu, K. Tokaji, *Fatigue Fracture Materials Structure*, 30 (2007), 143–148
- <sup>2</sup> P. C. Lin, J. Pan, T. Pan, *Journal Fatigue*, 30 (2008), 90–105
- <sup>3</sup> M. Merzoug, M. Mazari, L. Berrahal, A. Imad, *Materials Design*, 31 (2010), 3023–3028
- <sup>4</sup> Y. C. Chen, K. Nakata, *Materials Design*, 30 (2009), 3913–3919
- <sup>5</sup> M. I. Khan, M. L. Kuntz, P. Su, A. Gerlich, T. North, Y. Zhou, *Technology Welding Joining*, 12 (2007), 175–182
- <sup>6</sup> M. K. Bilici, A. I. Yukler, M. Kurtulmus, *Materials Design*, 32 (2011), 4074–4079
- <sup>7</sup> A. Arıcı, S. Mert, *Journal of Reinforce Plastics and Composite*, 1 (2008), 1–4
- <sup>8</sup> P. F. H. Oliveria, S. T. A. Filho, J. F. Santos, E. Hage, *Materials Letters*, 64 (2010), 2098–2101
- <sup>9</sup> M. K. Bilici, A. I. Yukler, *Materials Design*, 33 (2012), 145–152
- <sup>10</sup> Y. Tozaki, Y. Uematsu, K. Tokaji, *International Journal of Machine Tools and Manufacture*, 47 (2010), 2230–2236
- <sup>11</sup> N. Ma, A. Kunugi, T. Hirashima, K. Okubo, M. Kamioka, *Welding International*, 23 (2009), 9–14
- <sup>12</sup> M. Aydin, *Polymer Plastics Technology Engineering*, 49 (2010), 595–601
- <sup>13</sup> M. Awang, V. H. Mucino, Z. Feng, S. A. David, *SAE International*, 1 (2005), 1251–1256
- <sup>14</sup> S. J. Vijay, N. Murugan, *Materials Design*, 31 (2010), 3585–3589
- <sup>15</sup> H. M. Costa, V. D. Ramos, M. C. G. Rocha, *Polymer Testing*, 24 (2005), 86–93
- <sup>16</sup> C. Capone, L. D. Landro, F. Inzoli, M. Penco, L. Sartore, *Polymer Engineering Science*, 47 (2007), 1813–1819
- <sup>17</sup> S. T. Lim, C. A. Kim, H. Chung, H. J. Choi, J. H. Sung, *Korea-Australia Rheology Journal*, 2 (2004), 57–62
- <sup>18</sup> A. Gerlich, T. H. North, M. Yamamoto, *Science and Technology of Welding and Joining*, 12 (2007), 472–480
- <sup>19</sup> R. S. Mishra, Z. Y. Ma, *Materials Science Engineering*, 50 (2005), 1–78
- <sup>20</sup> Y. X. Gan, S. Daniel, *Materials*, 3 (2010), 329–350
- <sup>21</sup> W. Yuan, R. S. Mishra, S. Web, Y. L. Chen, B. Carlson, D. R. Herling, G. J. Grant, *Journal of Materials Processing Technology*, 211 (2011), 972–977
- <sup>22</sup> J. E. Mark, *Polymer Data Handbook*, Oxford University Press, New York 1999
- <sup>23</sup> S. M. Chowdhury, D. L. Chen, S. D. Bhole, X. Cao, *Materials Science Engineering A*, 527 (2010), 6064–6075